XL CILAMCE
IBERO-LATIN AMERICAN CONGRESS ON COMPUTATIONAL METHODS IN ENGINEERING
NOVEMBER 11-14, 2019
Praiamar Natal Hotel & Convention
Natal, RN-BRAZIL

APPLICATION OF INVERSE PROBLEMS ADDING VALUE TO CONTINUOUS MEASUREMENT DATA IN WELLS: THERMAL PROFILE OF REHEATING IN OIL RESERVOIRS

Victor Costa da Silva
vcsilva@petrobras.com.br
COPPE, University of Rio de Janeiro
PETROBRAS
Rua Henrique Valladares, 28, Torre B, 7th floor, Centro, Rio de Janeiro, Brazil

Paulo Couto
pcouto@petroleo.ufrj.br
COPPE, University of Rio de Janeiro
LIEP - Rua Moniz Aragão, 360, Bloco 4, Room 9, Cidade Universitária, Rio de Janeiro, Brazil

Franciane Conceição Peters
fran@coc.ufrj.br
COPPE, University of Rio de Janeiro
LAMEMO – Avenida Pedro Calmon, Bloco M, Cidade Universitária, Rio de Janeiro, Brazil

Abstract. The authors main objective in this work is to present, from different real conditions of the Braziliam Pres-Salt wells, under various operating conditions, and through complex numerical models and optimization tools and problems conversely as the temperature signatures can be considered for the injectable effect, while the active zone, as well as the saturation of the rest environments as well as the cooling of the same. This objective will be reached though the solution of an inverse problem, regarding linear optimization aiming the history matching process. The optimization will gives the pursued information, critical for the reservoir management.

Keywords: Thermal simulation, inverse problem, optimization, apportionment estimation

1 Introduction

Among others, reservoir management activity consists of acting reactively or proactively to undesired events for oil production activity, such as increase of WCUT or GOR in producing wells, due to injection of fluids in the respective injector pairs. Perhaps the greatest difficulty in this reaction is the traceability of the paths percolated by the injected fluids, both near the producing wells and the injector wells.

In simple completion wells (a single production or injection zone) it is possible to evaluate the well production/injection profile through direct gauging tools such as the production log test (PLT) at any time during well operation. Selective completion wells (whether intelligent or mechanical), the measurement via PLT, is only partially effective, as few well regions could be evaluated. In addition, the operation is risky and can generate fish in the column and eventually even compromise since the fulfillment of its economic function.

However in Intelligent Completion (IC) wells, annular permanent downhole gauges (PDG), through their temperature data, represent an important tool for tracking, at least in a macro way, the saturation modification in each evaluated section. Evaluating injector wells shows three distinct propagation phenomena in the porous environment: (i) pressure propagation; (ii) propagation of injection fluid saturation; and (iii) temperature propagation, since injection occurs at temperatures lower than the reservoir static. Due to the flow conditions and equations that govern each one, it can be expected that for each time: x_lim (pressure) > x_lim (Saturation)> x_lim (Temperature), since the temperature propagation occurs before a reservoir of infinite global thermal capacity.

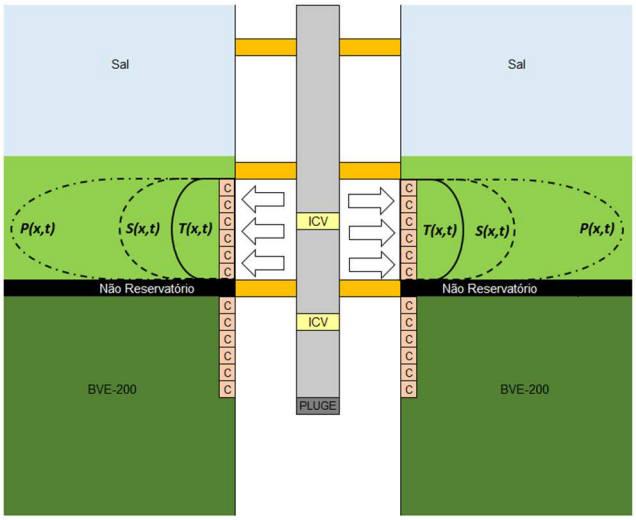

Figure 1 - Schematic representation of pressure, saturation and temperature wave propagation in porous media from an injector well

This work aims to bring, from real data from wells of PPSBS (Santos Basin Pre-Salt Pole), under different operational conditions, to study the phenomenon that presents itself, and through complex numerical models and optimization and optimization tools. Inverse problems identify how some heating signatures can indicate how much injected fluid has passed through each zone effectively, either by changing the saturation of the well surroundings or cooling it.

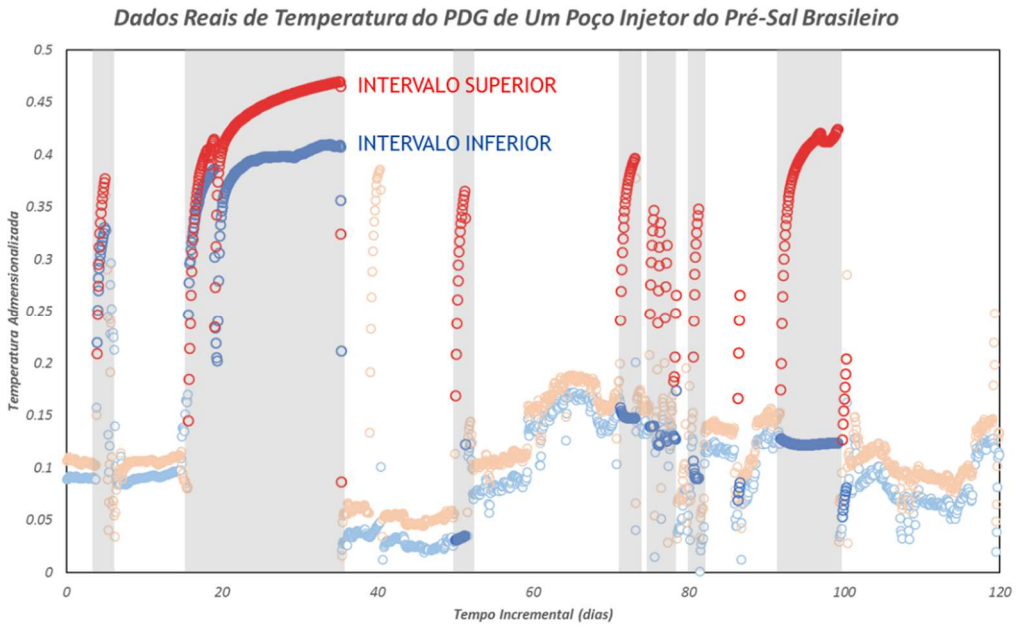

Figure 2 - Actual heating data of an injector well with individualized temperature measurements at 2 reservoir points.

2 Mathematical Modelling

In order to better evaluate the well-reservoir coupling will be used a radial grid and relevant properties evenly distributed throughout the cells. As a simplification, each interval of interest was not vertically discretized, since the reservoir in this interval would be considered vertically homogeneous and the coupling with the well would occur by a single point.

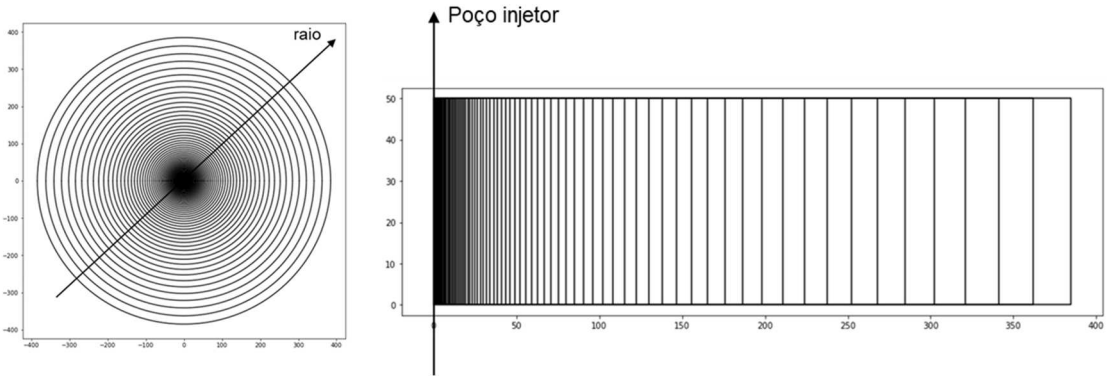

Figure 3 - Schematic diagrams of the well-reservoir coupling model in radial coordinates, applied to solve the proposed problem.

Any measurement of the disturbed region from the temperature data of the annular PDGs should be performed in static mode due to the lower data noise. Despite this static approach, which could imply a flowless regime in the porous environment and, consequently, suppress some relevant terms in the equation of the energy balance equation, this work proposes to follow with the complete modeling, with all the relevant terms, are they:

1. Transient Effect
2. Thermal conductivity
3. Advection

4. Compression
5. Viscous Dissipation
6. Thermal Coupling Between Intervals

Therefore the energy balance equation (EBE) is rewritten as:

$$cp_j\rho_j\frac{\partial\theta_j(r_j,t)}{\partial t} = -k_j\frac{\partial\theta_j^2(r_j,t)}{\partial^2 r_j} + cp_j\rho_j v_{r_j}(r_j,t)\frac{\partial\theta_j(r_j,t)}{\partial r_j} + \beta_j\phi_j\theta_j(r_j,t)\frac{\partial P_j(r_j,t)}{\partial t} + \Delta z_j v_{r_j}(r_j,t)\frac{\partial P_j(r_j,t)}{\partial t}\left[\beta_j\theta_j(r,t)-1\right] + \pi\left(r_i^2 - r_{i-1}^2\right)k_{12}\frac{\left(\theta_{j=2}-\theta_{j=1}\right)}{2\Delta z} \quad (1)$$

In the above equation the superscript j represents the range of interest, which may be 1 (upper) or 2 (lower). The term k_{12} represents the thermal conductivity of the so-called "non-reservoir" range. Finally it is possible to discretize the above equation into cylindrical coordinates, to better represent the geometry close to the injector well of interest. Thus we will have:

$$cp_j\left[\frac{cp_j\,\rho_j}{2\Delta r}v_{r_{i,j}}^{tn} - \left(1-\frac{1}{2i}\right)\frac{k_j}{\Delta r^2}\right]\theta_{r_{i-1,j}}^{tn} + \left[\frac{cp_j\rho_j}{\Delta t} - 2\frac{k_j}{\Delta r^2} - \frac{\beta_j\phi_j}{2\Delta t}\left(P_{r_{i+1,j}}^{tn} - P_{r_{i-1,j}}^{tn}\right) - \frac{\Delta z_j\beta_j v_{ri_1}^{tn}}{2\Delta r}\left(P_{r_{i+1,j}}^{tn} - P_{r_{i-1,j}}^{tn}\right) + k_{12}\right]\theta_{r_{i,j}}^{tn} + \left[-\frac{cp_j\,\rho_j}{2\Delta r}v_{r_{i,j}}^{tn} + \left(1+\frac{1}{2i}\right)\frac{\lambda}{\Delta r^2}\right]\theta_{r_{i+1,j}}^{tn} = \left[-\frac{cp_j\,\rho_j}{\Delta t}\theta_{r_{i,j}}^{tn-1} + \frac{\Delta z\beta_j v_{r_{i-1,j}}^{tn}}{2\Delta r}\left(P_{r_{i-1,j}}^{tn} - P_{r_{i-1,j}}^{tn}\right) + k_{r_i12}\theta_{ri,j*}^{tn}\right] \quad (2)$$

Summing up term by term we have:

- cp = thermal capacity at constant pressure
- ρ = desnsity
- $v_{ri,j}^{tn}$= fluid velocity in the porous medium of radius i in layer j and time n
- k = termal conductivity
- β = thermal expansion coefficient
- $p_{r_{i,j}}^{tn}$ = porous media pressure of radius i at layer j and at time n
- Δz_j = thickness of layer j
- $\theta_{r_{i-1,j}}^{tn}$ = porous media temperature of radius i in layer j and time n
- $k_{ri_{12}} = \pi\left(r_i^2 - r_{i-1}^2\right)k_{12}/2\Delta z$ = thermal conductivity between layers 1 and 2
- $\theta_{ri,j*}^{tn}$ = porous medium temperature at radius i in the layer adjacent to j (j *) in time *tn*

To estimate the pressure fields, the numerical solution of the hydraulic diffusivity equation (HDE) will be applied and, from this, the velocity fields will be obtained. Below I highlight the equation of the EDH and the velocity field.

$$cp_j\frac{\partial^2 P(r,t)}{\partial r^2} = \frac{\phi\mu(\theta)c_t(\theta)}{k}\frac{\partial P(r,t)}{\partial t} \quad (3)$$

In cylindrical coordinates the above equation will be discretized as:

$$\left(1+\frac{1}{2i}\right)P_{r_{i+1}}^{tn} - 2P_r^{tn} + \left(1-\frac{1}{2i}\right)P_{r_{i-1}}^{tn} = a\frac{\Delta r^2}{\Delta t}\left(P_{ri}^{tn+1} - P_{ri}^{tn}\right) \quad (4)$$

where $a = \phi\mu c_t/k$.

$$v_{ri}^{tn} = \frac{k/\mu}{2\pi r_i \Delta z}\left[\left(\frac{\partial P}{\partial r}\right)_{r_{i-\frac{1}{2}}}^{tn} - \left(\frac{\partial P}{\partial r}\right)_{r_{i+\frac{1}{2}}}^{tn}\right] \tag{5}$$

Discreting the above equation in cylindrical coordinates we have the following solution:

$$v_{ri}^{tn} = -\frac{k/\mu}{2\pi r_i \Delta z \Delta r}\left[P_{r_i+1}^{tn} - 2P_{r_i}^{tn} + P_{r_i-1}^{tn}\right] \tag{6}$$

The thermal properties of the reservoir, which are a function of the temperature and pressure field, must be updated with each new timestep. In addition, as the proposed problem advocates multiphase flow, the properties in question also depend on the saturation field, being obtained from the weighted averages below.

$$cp_{t_{ri}}^{tn} = \phi_{r_i} o_{ri}.\, cp_o(\theta^{tn-1}, P^{tn-1}) + (1 - So_{ri}).\, cp_{inj}(\theta^{tn-1}, P^{tn-1}) + \left(1 - \phi_{r_i}\right) cp_{rocha} \tag{7}$$

$$\rho_{t_{ri}}^{tn} = \phi_{r_i} o_{ri}.\, \rho_o(\theta^{tn-1}, P^{tn-1}) + (1 - So_{ri}).\, \rho_{inj}(\theta^{tn-1}, P^{tn-1}) + \left(1 - \phi_{r_i}\right) \rho_{rocha} \tag{8}$$

$$k_{t_{ri}}^{tn} = \phi_{r_i} o_{ri}.\, k_o(\theta^{tn-1}, P^{tn-1}) + (1 - So_{ri}).\, k_{inj}(\theta^{tn-1}, P^{tn-1}) + \left(1 - \phi_{r_i}\right) k_{rocha} \tag{9}$$

3 Workflow e Direct Problems Results

The workflow to obtain the solution of the direct problem will be based on the definition of the initial saturation temperature fields that will feed the equations and the numerical process highlighted above. It is shown below.

1 - Definition of constant properties along the simulation grid for both intervals;

2 - Definition of the initial pressure condition for both intervals;

3 - Definition of the initial temperature condition for both ranges;

4 - From (2) set the initial saturation condition for both intervals

5 - Estimation of variable properties in P and T;

6 - From (1), (2) and (5) obtain implicit numerical solution of the EDH to obtain the pressure field at both intervals;

7 - From (1), (5) and (6) obtain the velocity field at both intervals;

8 - From (1), (3), (5), (6) and (7) obtain the implicit numerical solution of EBE to obtain the temperature field for each interval. In this step it is important to detail that, as proposed, there is a thermal coupling between intervals 1 and 2 and, therefore, the EBE solution will also require (3) the coupled layer;

9 - Feedback (2) with (8) and follow the flow to the next timestep;

It is noteworthy that obtaining the saturation field from the initial temperature field, by itself, is already a conceptual challenge. The saturation field is very important for the development of this work because (i) it will both serve as a basis for the estimation of the average parameters that will be used in the Energy Balance Equation and (ii) will be our fundamental parameter to estimate the fraction of the energy. total flow rate that was injected at each of the ranges of interest.

(i) We will observe in the following sections how the saturation field influences the thermomechanical parameters involved in the coupled approach between EDH and EBH in order to obtain the final product that corresponds to the evolution of the temperature field in the reservoir over time.

(ii) We know that all the volume injected into the reservoir causes the displacement of the oil, originally present in the formation, being replaced by the injected fluid, in this case water. So there is an obvious correlation between the reservoir water saturation field and the volume that was originally injected at each interval, namely:

$$Vw_{inj} = 2\pi\Delta z \int \phi\, Sw(r)\, r\, dr \tag{10}$$

Discrete for the grid we are working on we will have:

$$Vw_{inj} = \pi\Delta z \sum Sw_i\, \phi_{r_i} \Delta r_i^2 \tag{11}$$

Therefore, from the saturation field, we would easily have the injected flow fractions in each interval through:

$$x_1 = \frac{Vw_{inj_1}}{Vw_{inj_1} + Vw_{inj_2}} \tag{12}$$

$$x_2 = \frac{Vw_{inj_2}}{Vw_{inj_1} + Vw_{inj_2}} \tag{13}$$

However, it is intuitive to think that the injected fluid saturation field is linearly dependent on the initial temperature field it generates in the reservoir. This is because what causes cooling in the system during injection is exactly the percolation of cold fluid in the reservoir, so the larger the volume of injected fluid, the greater the system cooling, and the greater the water saturation in the reservoir. . Therefore there must be a constitutive relationship between these 2 quantities, but which is not known a priori.

In literature the author was not successful in identifying such constitutive relationship, so that 2 options were presented:

a. Obtain this relationship through the coupling of EBE and EDH to the flow regime, as well as the Buckley-Leverett model;
b. Generate, through STARTS commercial software, representation of the proposed grid and simulate several injection flow levels, for the same time period, and directly obtain the generated saturation and temperature fields. And, from these results, generate the desired constitutive relationship.

In order not to significantly increase the scope of this paper, alternative (b) was chosen. With this alternative we guarantee that the Buckley-Leveret model will be respected and much less laborious to obtain. The graph below shows the relationship between normalized temperature and normalized saturation, resulting from 4 of the above simulations.

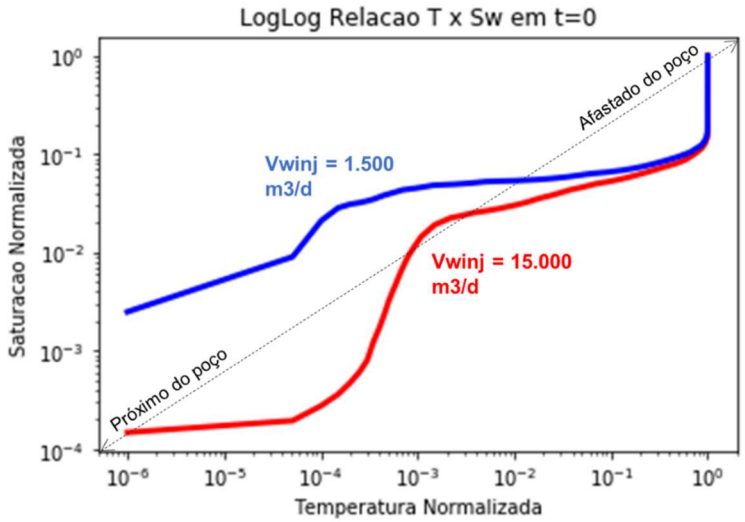

Figure 4 - Constitutive relationship between reservoir cooled front temperature and saturation field at the end of the flow period

Note that the author used the concept of normalized temperature and saturation. This is due to the desire to adequately represent both variables on the same scale and with representative coherence. Such normalizations were applied as below.

$$\theta_{norm} = \frac{\theta - \theta_{inj}}{\theta_{\infty} - \theta_{inj}} \tag{14}$$

$$Sw_{norm} = \frac{Sw - (1 - Sor)}{1 - Swi - Sor} \tag{15}$$

As presented both variables tend to zero while $r \to 0$ and tends to 1,0 when $r \to r_{\infty}$.

It is highlighted in the graph above that the constitutive relationship between temperature and saturation is not unique, as one might think at first, but varies according to the imposed flow level. This is because in the high flow rates the higher flow implies the advective and thermal diffusion regimes, governed by turbulence and responsible, in relation to the conductive regime. This causes less time available for the injected cold mass to gain heat from the reservoir, and thus the cold front advances more rapidly in the middle. For low flow rates, the opposite is true, with heat exchange occurring rapidly, thus restricting the advance of the cooled front in the reservoir.

From what has been presented here it is reasonable to assume that for a given temperature field there is only one corresponding saturation field (assuming that the only relevant variable that the problem adopts is the flow rate). In contrast to the same saturation field we may have different temperature fields. Thus the author assumes that the constitutive relationship between normalized saturation and normalized temperature will be a function of the temperature field itself.

Therefore, from the workflow presented above and the development of the correlation between temperature and saturation as above, it is possible to implement, for a given initial temperature condition, what would be its evolution over time in static regime for the 2 evaluated intervals. The initial temperature condition in question is given by:

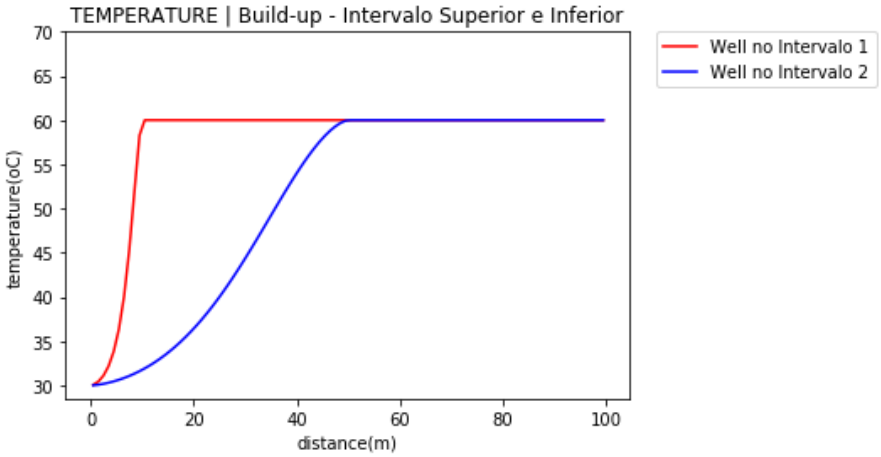

Figure 5 - Initial condition of temperature field for both ranges of interest

For this condition we will have the evolution of the temperature field in the two intervals over time as below:

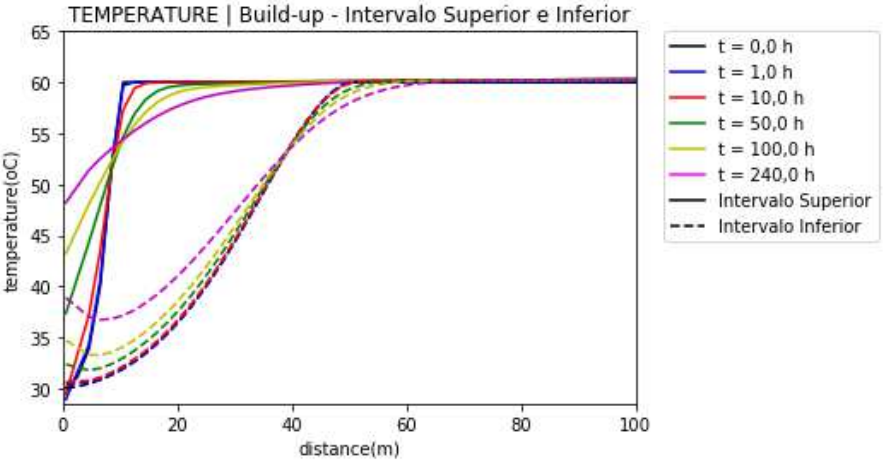

Figure 6 - Evolution of temperature over the static period for different times. Full lines represent evolution in the Upper Interval (1) and dotted line in the Lower Interval (2)

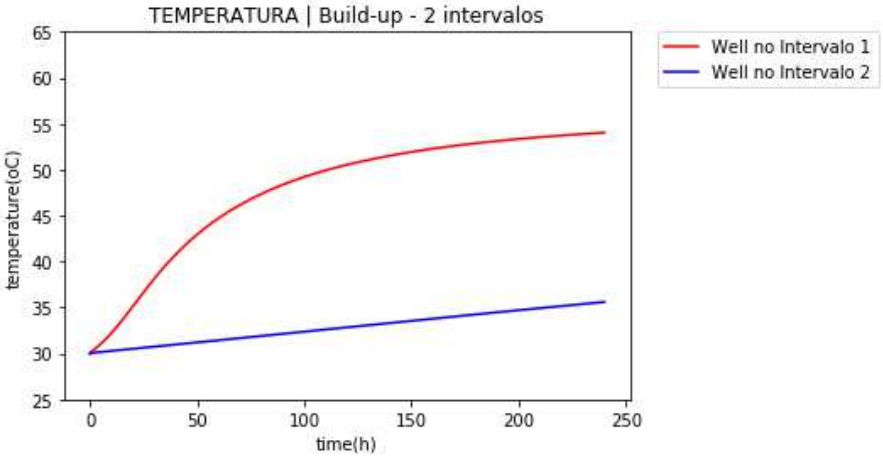

Figure 7 - Evolution of the temperature over the static period in the well position, equivalent to the data effectively available for historical adjustment.

4 Workflow e Resultados do Problema Inverso

Once presented and discussed the proposed numerical model for solving the direct problem we will move on to this chapter to discuss the results of the temperature field as a result of flow simulation and obtained directly from real data from injector wells of Brazilian pre-salt fields.

The synthetic data were obtained from a simulated representative flow model in the STARS 2017.1 software of CMG suite. This thermal flow simulator allows us to evaluate the thermal behavior of an oil reservoir when subjected to cold fluid injection, in order to evaluate how the heating profile of the reservoir would be static. The 4 scenarios that were evaluated had the flow distribution as below.

Table 1. Fração Injetada em Cada Intervalo – Simulação Numérica

Scenario	X(%) Upper Interval	X(%) Lower Interval
1	16,7%	83,3%
2	72,5%	28,5%
3	2,0%	98,0%
4	66,7%	33,3%

Due to the complexity of the solution that would be imposed if the initial grid temperature field is to be obtained directly, that is, with the temperature of each cell being a variable to be determined, besides increasing the degree of uniqueness of the solution, It was proposed that the definition of the initial temperature field be obtained in a parameterized way, through the function below.

$$\frac{\theta(x)-\theta_{wf}}{\theta_{\infty}-\theta_{wf}}=\frac{\left(\frac{r}{R_{\infty}}\right)^{a}}{\left(\frac{r}{R_{\infty}}\right)^{a}+b\left[1-\left(\frac{r}{R_{\infty}}\right)\right]^{a}}=f(r,a,b,R_{\infty}) \tag{16}$$

Thus the solution of the inverse problem will be given from the definition of the 3 parameters above for each range of interest, ie:

$$m=\begin{bmatrix}\theta^{1}\\ \theta^{2}\end{bmatrix}_{t=0}^{r}=\begin{bmatrix}\theta_{1}^{1} & \theta_{2}^{1} & \dots & \theta_{n}^{1}\\ \theta_{1}^{2} & \theta_{2}^{2} & \dots & \theta_{n}^{2}\end{bmatrix}_{t=0}^{r}\rightarrow m=\begin{bmatrix}\theta^{1}\\ \theta^{2}\end{bmatrix}_{t=0}^{r}=\begin{bmatrix}a^{1} & b^{1} & R_{\infty}^{1}\\ a^{2} & b^{2} & R_{\infty}^{2}\end{bmatrix} \tag{16}$$

This definition, in addition to reducing the degree of complexity of obtaining the inverse problem, accelerating convergence, also reduces the degree of solution unity.

The simulated heating profiles for the 4 scenarios above are reflected below. Such simulated data will be the reference to obtain the inverse problem and, later, definition of the injected fraction in

each interval.

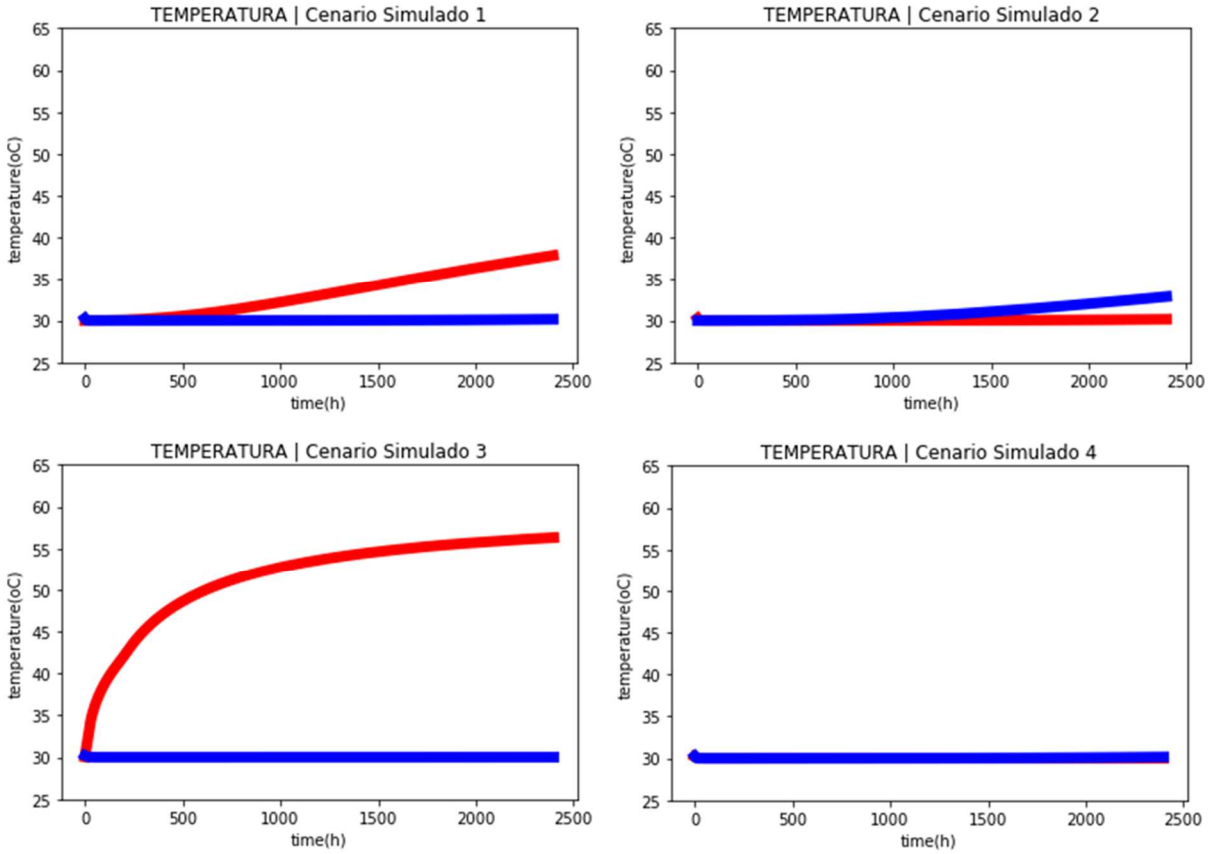

Figure 9. Data simulated from STARS Commercial Thermal Simulator, which will be used as exact data for inverse problem application

Once the concepts relevant to the inverse problem have been defined, as well as the linear programming method that was applied in this work, the last step to be detailed before the effective application of the proposed method to solve the inverse problem for the 4 synthetic data scenarios and for The 3 actual data sets, presented in sections 6.1 and 6.2, is the concatenation of these steps in the following workflow.

1 - Define the initial estimate for the 6 parameters that make up the solution of the inverse problem (a^1, b^1, R^1inf, a^2, b^2 and R^2inf).

2 - From (1) determine the initial temperature field

3 - From (1) and (2) determine the initial saturation field

4 - From (2) and (3) determine the variation of the temperature field over time through the workflow presented in section 5.2.

5 - From (4) calculate the residue function;

6 - Evaluate the residue value against the imposed tolerance. If it is smaller to break the loop;

7 - Update the parameters that make up the solution of the inverse problem through the Nelder-Mead method and return to (2)

Below is the evolution of the process of obtaining the inverse problem solution for each of the scenarios above. This process will be presented through the evolution of the residue, as well as the solution adjustment obtained with the data.

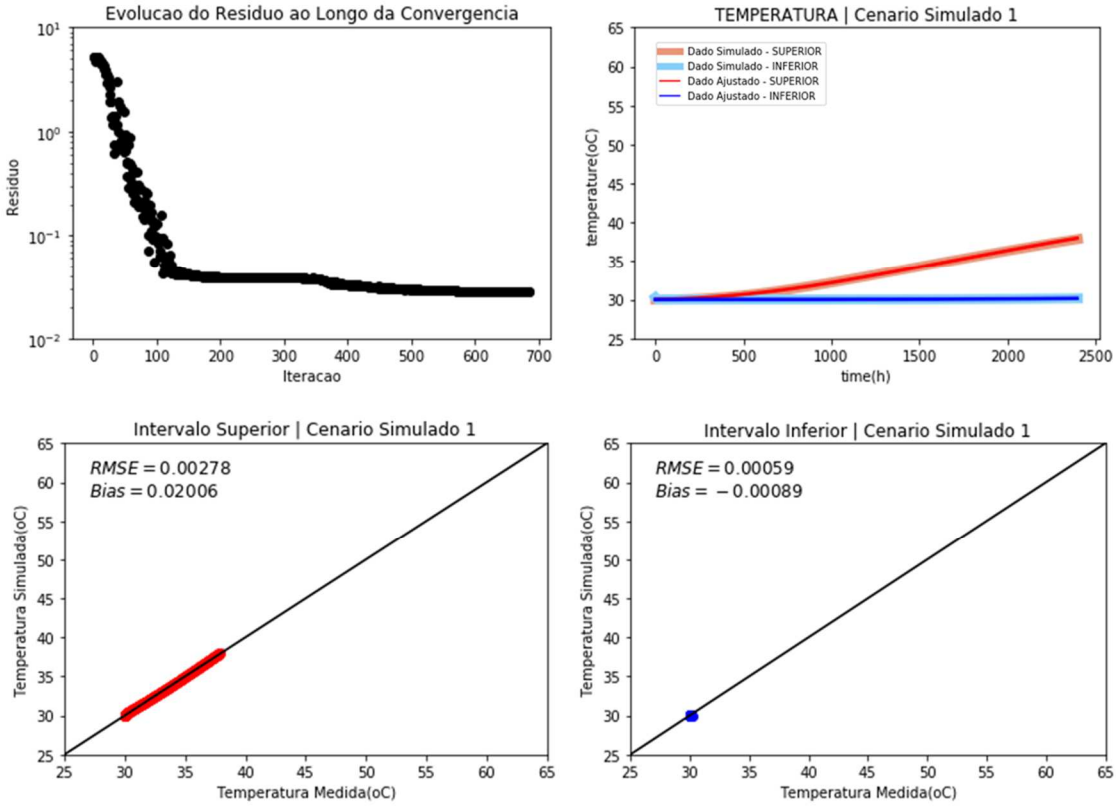

Figure 10. Inverse Problem Solution Obtained for Scenario 1

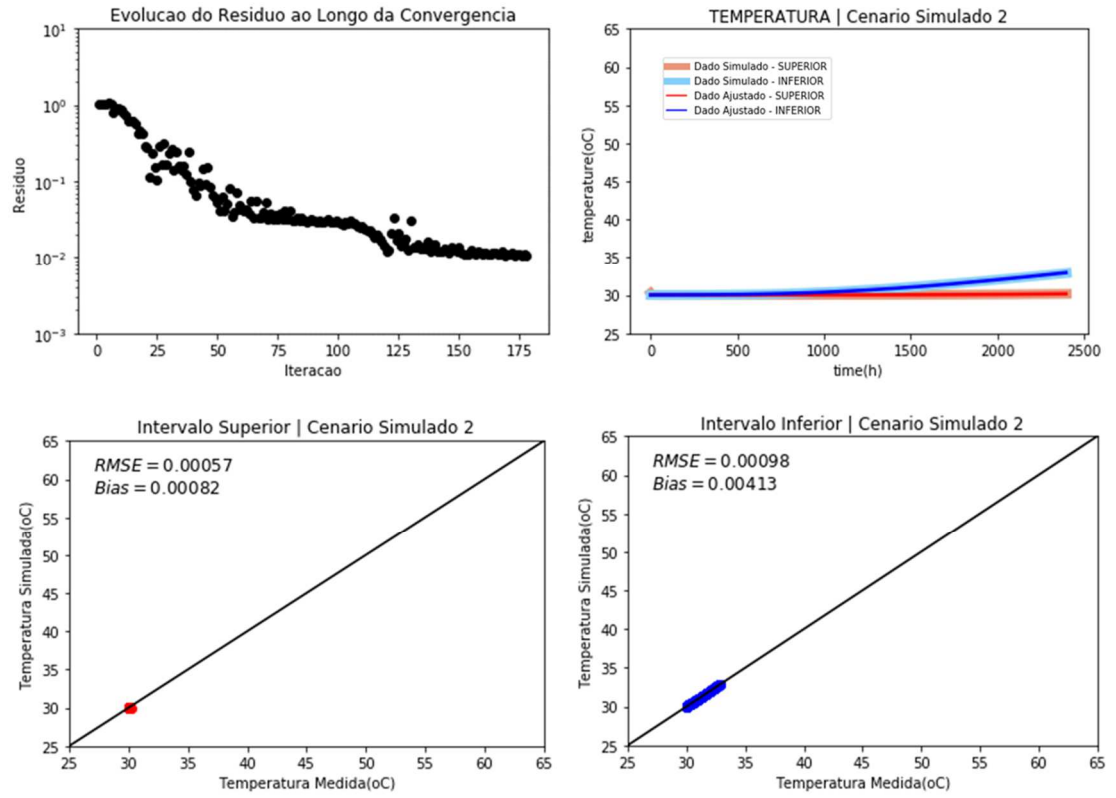

Figure 11. Inverse Problem Solution Obtained for Scenario 2

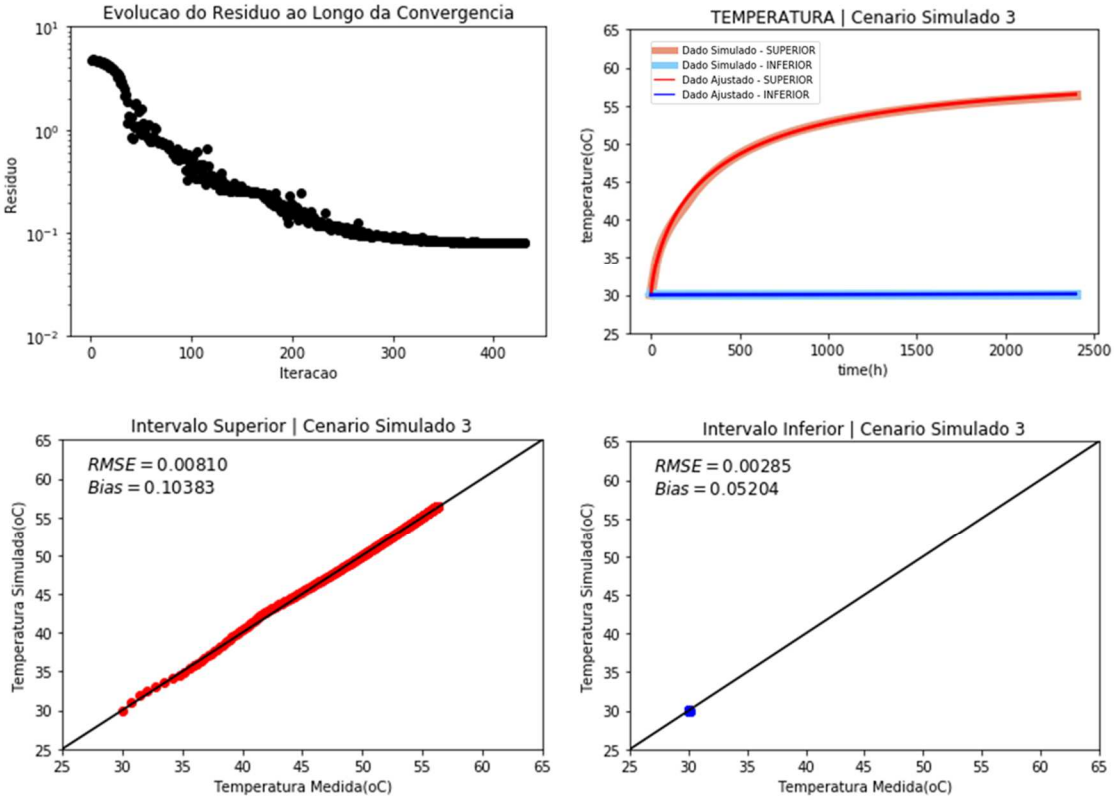

Figure 12. Inverse Problem Solution Obtained for Scenario 3

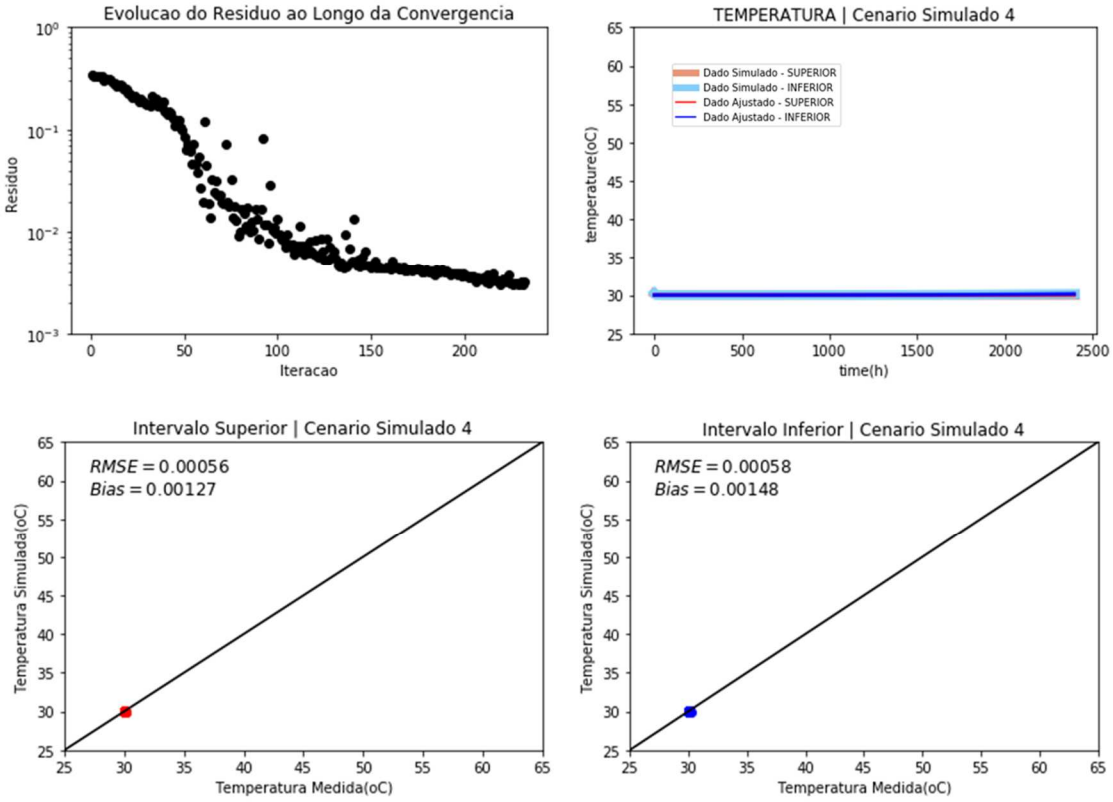

Figure 13. Inverse Problem Solution Obtained for Scenario 4

From the solutions obtained each of the scenarios in question and the workflow that was presented previously it is possible to determine which equivalent saturation field is present in each interval and, consequently, which fraction of the injected volume that percolated each of the intervals of interest. The figure below shows the 4 saturation fields obtained for the 4 scenarios.

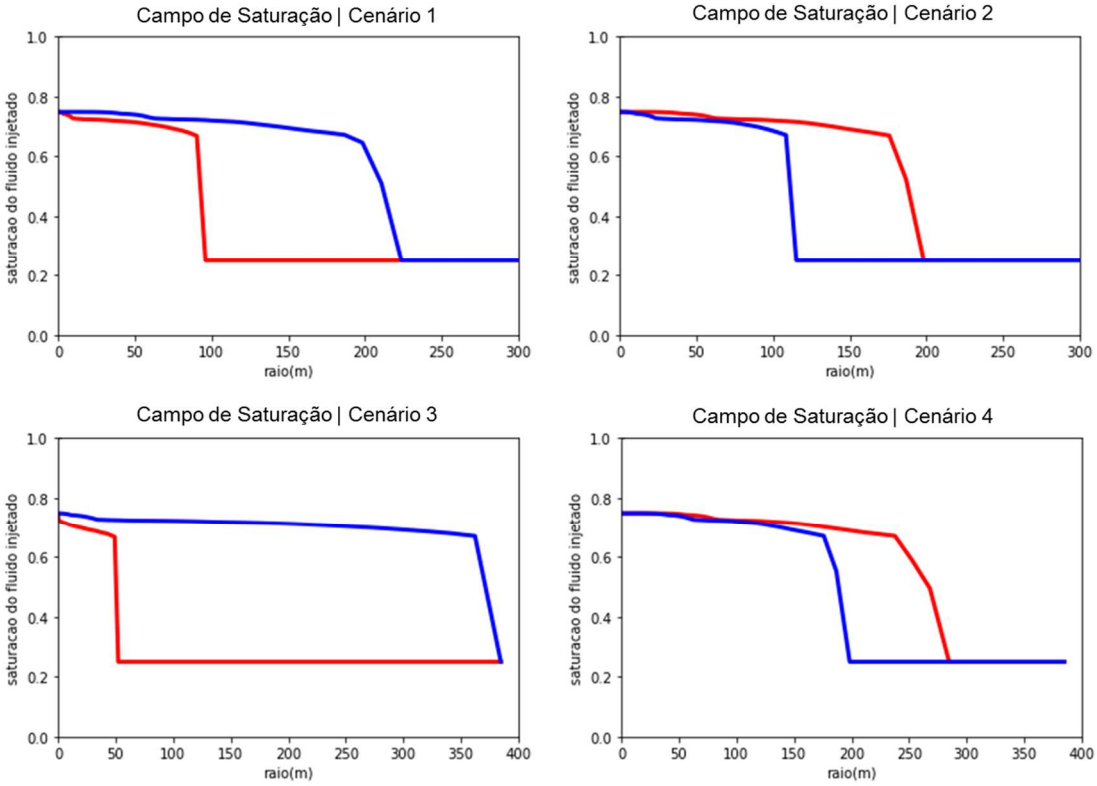

Figure 14. Injection saturation field obtained from the inverse problem solution

The table below summarizes all results obtained from the inverse problems solved for each of the 5 simulated scenarios in STARS commercial software. It is important to note the low RMSE and Bias values of the solutions obtained, as well as the low deviations from the predicted ratios against the exact data.

Tabel 2. Summary of Data Inverse Problem Solution Matching

Scenario	**Residue**	**RMSE**	**Bias**	**% Deviation Rateio Apportionment**
1	2,8E-2	1,7E-3	1,0E-2	0,4%
2	1,0E-2	7,8E-4	2,5E-4	1,4%
3	8,0E-2	5,5E-3	7,6E-2	0,1%
4	3,2E-3	5,7E-4	1,4E-3	0,4%

5 Conclusion

From the results of the 4 synthetic scenarios obtained from the commercial software STARS, it is proved that the proposed model is robust both for the definition of the injected flow rate and for the study of the phenomenon in question. All scenarios presented residuals below 0.01 and, when estimating

the injection ratio at each interval, the deviations were not greater than 1.5%. In addition, the Bias and RMSE estimates also prove a very precise adjustment of the inverse problem solution against the exact data.

Another important conclusion of this work is the confirmation of the initial suspicion that the static temperature signature in injector wells is a strong indication about the saturation profile of the injected fluid in the reservoir. With this work we understand a phenomenon not explored in the literature and we can extract from this information the maximum value that it could provide.

Acknowledgements

I acknowledge professors Paulo Couto and Franciane Peters for the rich orientation they gave to this work, from the theme to the results. I also thank Petrobras for the opportunity granted to do the master's degree and to publish this work and to CAPES for the incentive to the investment and the scientific publication.